**Supplementary Information for:**

# Unusual interlayer coupling in layered Cu-based ternary chalcogenides $CuMCh_2$(M=Sb, Bi; Ch=S, Se)

Dan-Dong Wang,[†] Xin-Gao Gong,[†§‡*] and Ji-Hui Yang[†‡*]

[†]Key Laboratory of Computational Physical Sciences (Ministry of Education), State Key Laboratory of Surface Physics, and Department of Physics, Fudan University, Shanghai 200433, China

[‡]Shanghai Qi Zhi Institute, Shanghai 200232, China

[§]Collaborative Innovation Center of Advanced Microstructures, Nanjing 210093, China

*corresponding author

Email: jhyang04@fudan.edu.cn; xggong@fudan.edu.cn

## 1. The phonon spectrum of $CuSbS_2$ monolayer and bilayer.

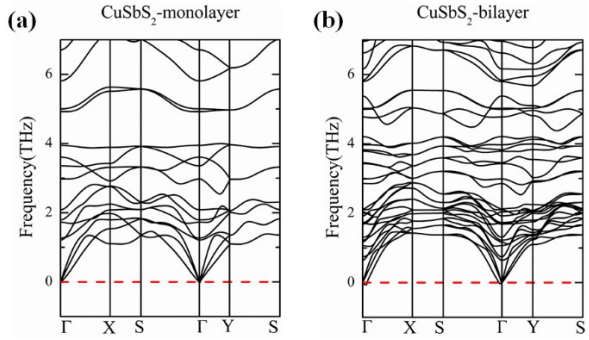


**Figure S1.** The phonon spectrum of $CuSbS_2$ (a) monolayer and (b) bilayer.

**2. HSE calculated band structure of $CuSbS_2$ monolayer.**

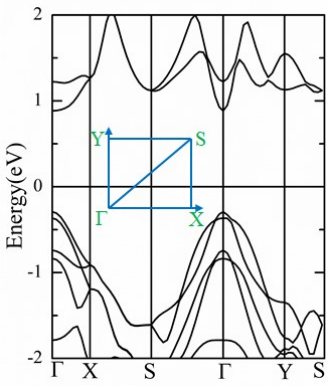


**Figure S2.** HSE band structure (see the blue inset for the high symmetrical K-points) without the spin-orbit coupling for monolayer $CuSbS_2$ where the Fermi level has been set to 0 eV.

**3. The optical absorption spectra of in $CuSbS_2$ monolayer and $CuSbSe_2$ monolayer.**

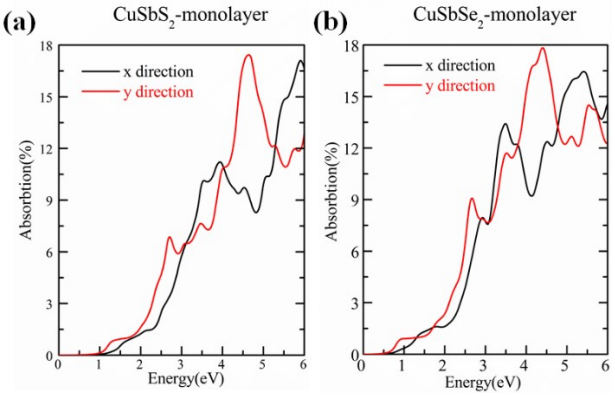


**Figure S3.** The optical absorption spectra of (a) $CuSbS_2$ monolayer and (b) $CuSbSe_2$ monolayer.

**4. Band alignments from the $CuSbS_2$ monolayer to four layers.**

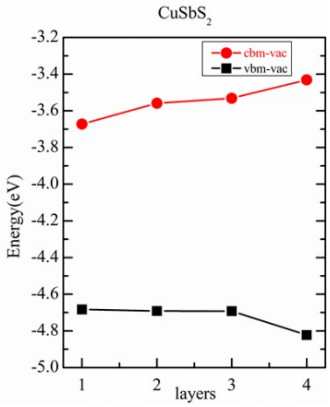


**Figure S4.** The band edge positions changes with same lattice constants from the $CuSbS_2$ monolayer to four layers by using the vacuum level as a common reference. The 'vbm-vac' means the VBM minus the vacuum level, and the 'cbm-vac' means the CBM minus the vacuum level.

**5. Structures, electronic structures, and atomic orbital projected band structures in $CuMCh_2$(M=Sb, Bi; Ch=S, Se)**

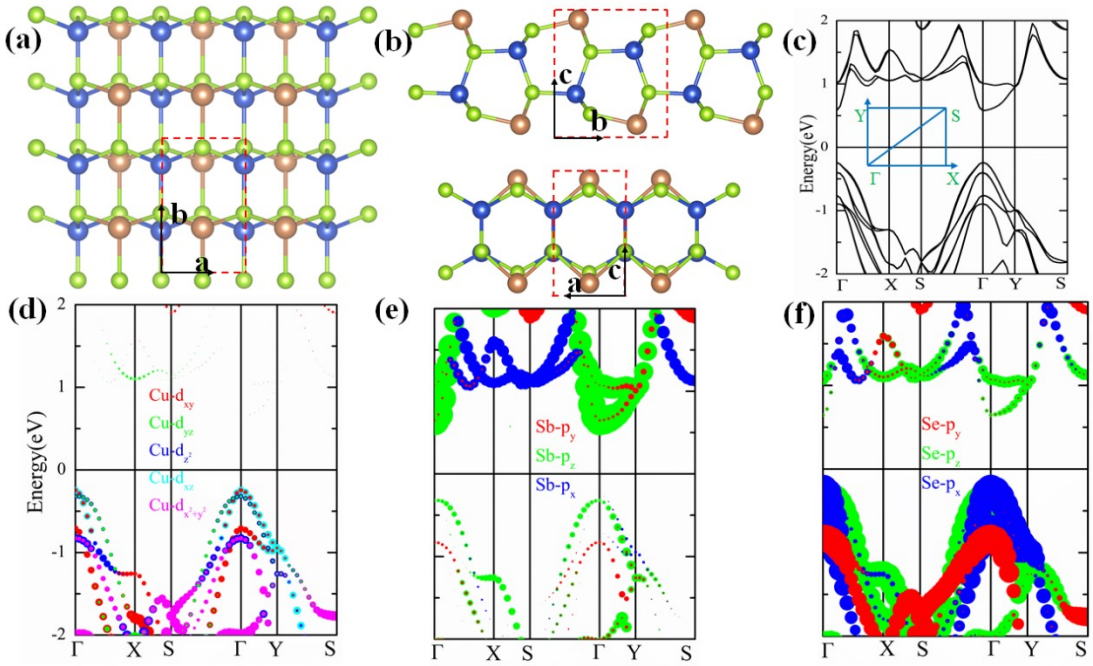


**Figure S5.** The structure, band structure, and atomic orbitals of the monolayer $CuSbSe_2$. (a) and (b) are the top and side views respectively. (c)HSE energy band structure calculations (see the blue inset for the high symmetrical K-points) with the spin-orbit coupling and Van der Waals interactions, where the Fermi level has been set to 0 eV. (d), (e) and (f) are atomic orbital projected band structures in Cu, Sb, Se atoms respectively. The Cu, Sb, Se atoms are shown as blue, brown and green spheres, respectively.

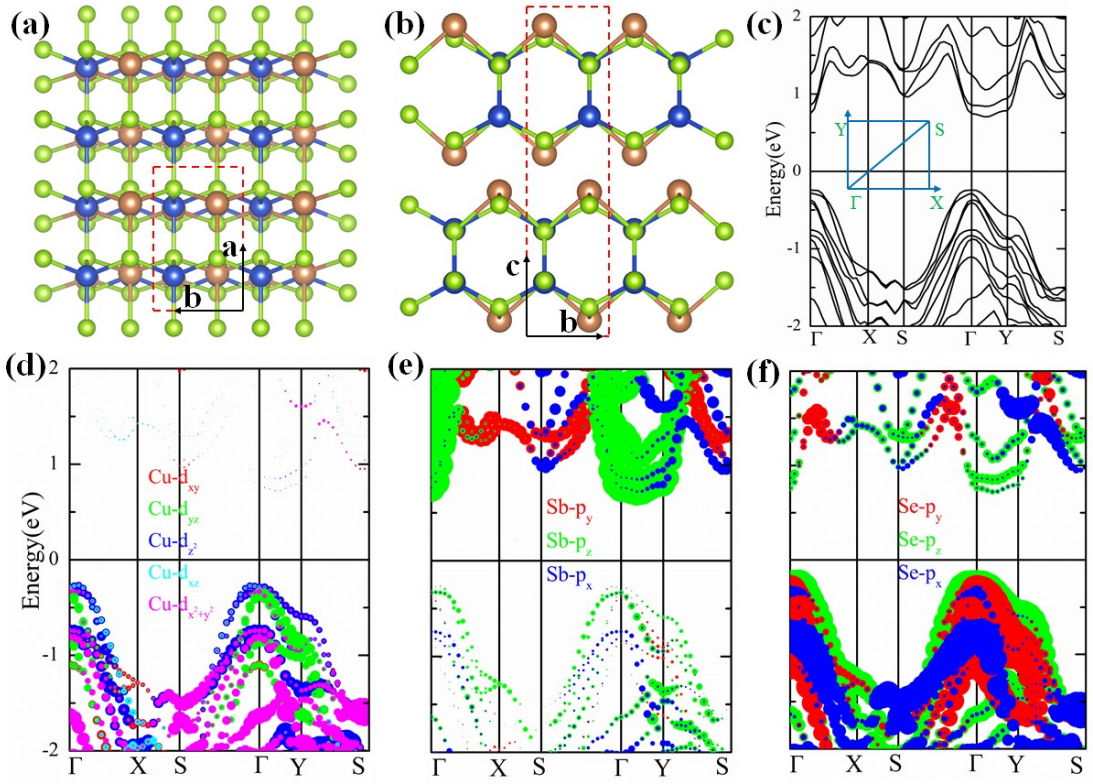


**Figure S6.** The structure, band structure, and atomic orbitals of the bilayer $CuSbSe_2$. (a) and (b) are the top and side views respectively. (c)HSE energy band structure calculations (see the blue inset for the high symmetrical K-points) with the spin-orbit coupling and Van der Waals interactions, where the Fermi level has been set to 0 eV. (d), (e) and (f) are atomic orbital projected band structures in Cu, Sb, Se atoms respectively. The Cu, Sb, Se atoms are shown as blue, brown and green spheres, respectively.

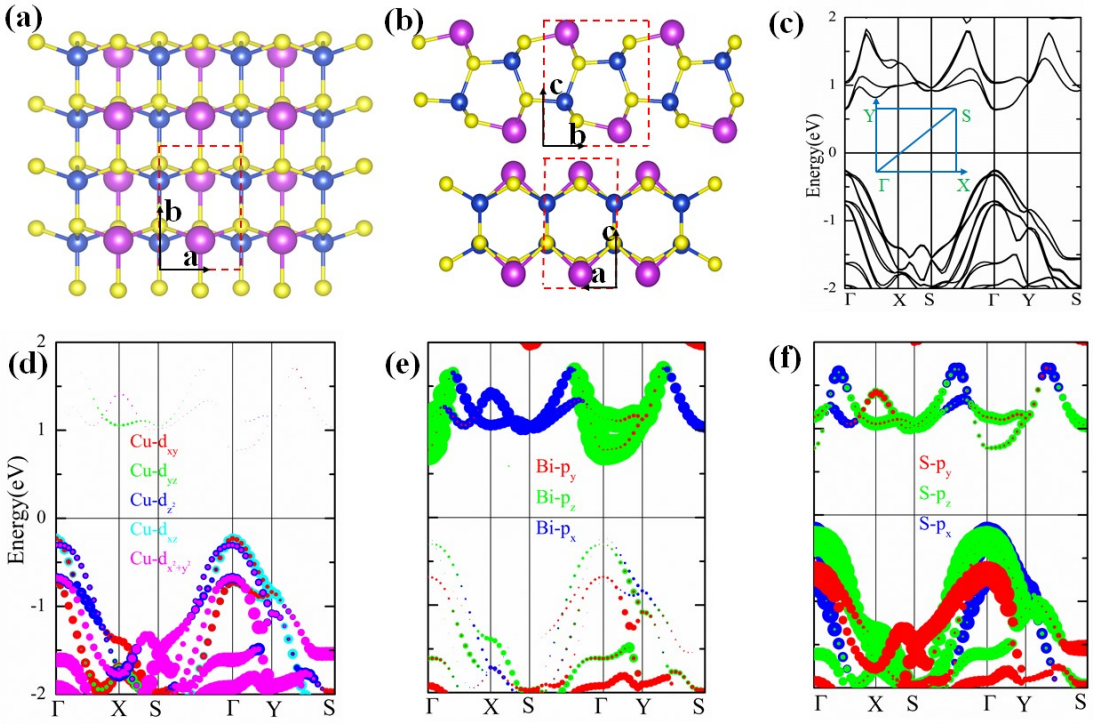


**Figure S7.** The structure, band structure, and atomic orbitals of the monolayer $CuBiS_2$. (a) and (b) are the top and side views respectively. (c)HSE energy band structure calculations (see the blue inset for the high symmetrical K-points) with the spin-orbit coupling and Van der Waals interactions, where the Fermi level has been set to 0 eV. (d), (e) and (f) are atomic orbital projected band structures in Cu, Bi, S atoms respectively. The Cu, Bi, S atoms are shown as blue, purple and yellow spheres, respectively.

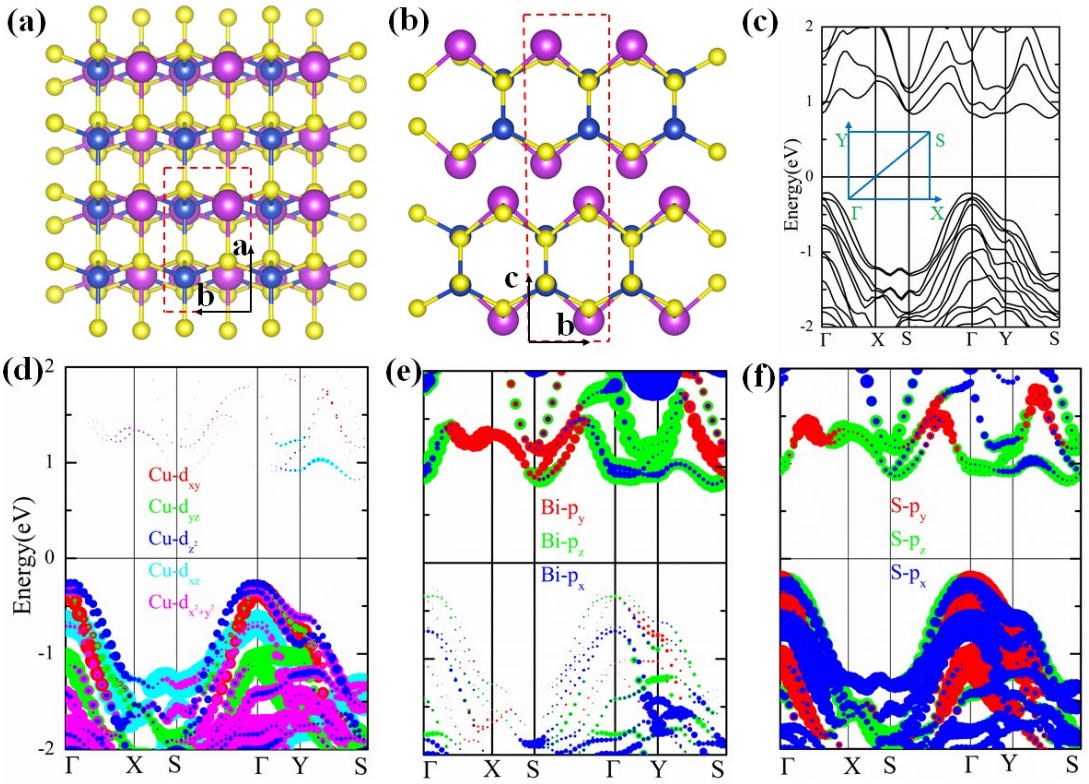


**Figure S8.** The structure, band structure, and atomic orbitals of the bilayer $CuBiS_2$. (a) and (b) are the top and side views respectively. (c)HSE energy band structure calculations (see the blue inset for the high symmetrical K-points) with the spin-orbit coupling and Van der Waals interactions, where the Fermi level has been set to 0 eV. (d), (e) and (f) are atomic orbital projected band structures in Cu, Bi, S atoms respectively. The Cu, Bi, S atoms are shown as blue, purple and yellow spheres, respectively.

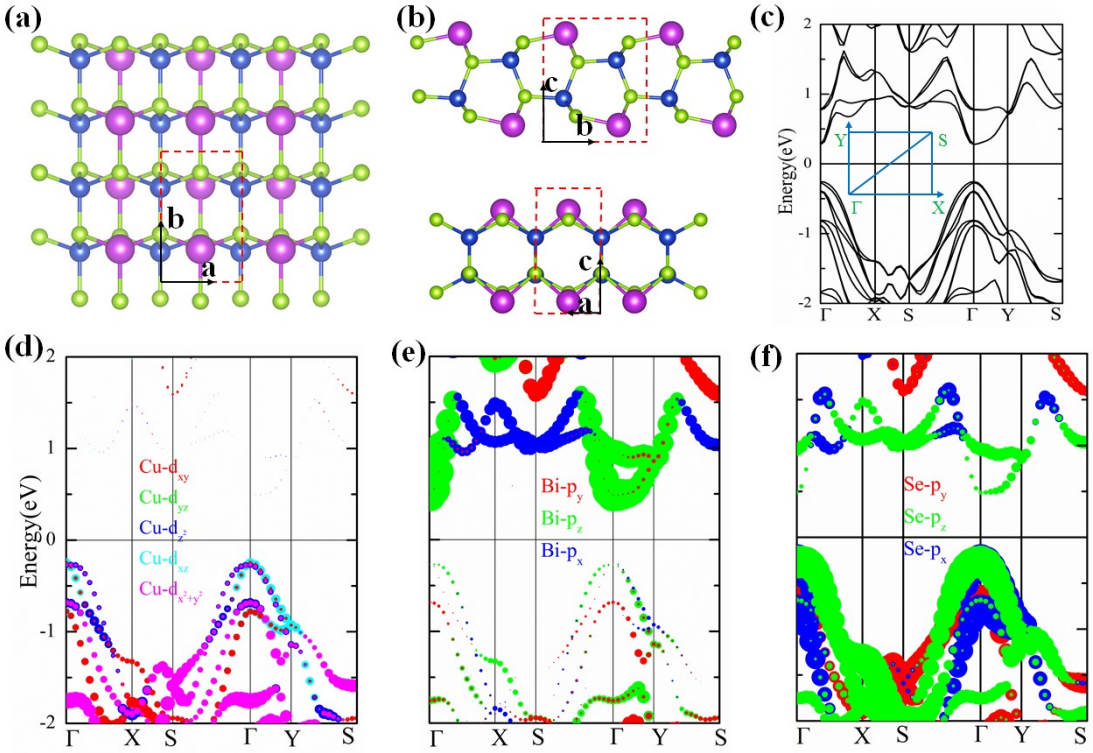


**Figure S9.** The structure, band structure, and atomic orbitals of the monolayer $CuBiSe_2$. (a) and (b) are the top and side views respectively. (c)HSE energy band structure calculations (see the blue inset for the high symmetrical K-points) with the spin-orbit coupling and Van der Waals interactions, where the Fermi level has been set to 0 eV. (d), (e) and (f) are atomic orbital projected band structures in Cu, Bi, Se atoms respectively. The Cu, Bi, Se atoms are shown as blue, purple and green spheres, respectively.

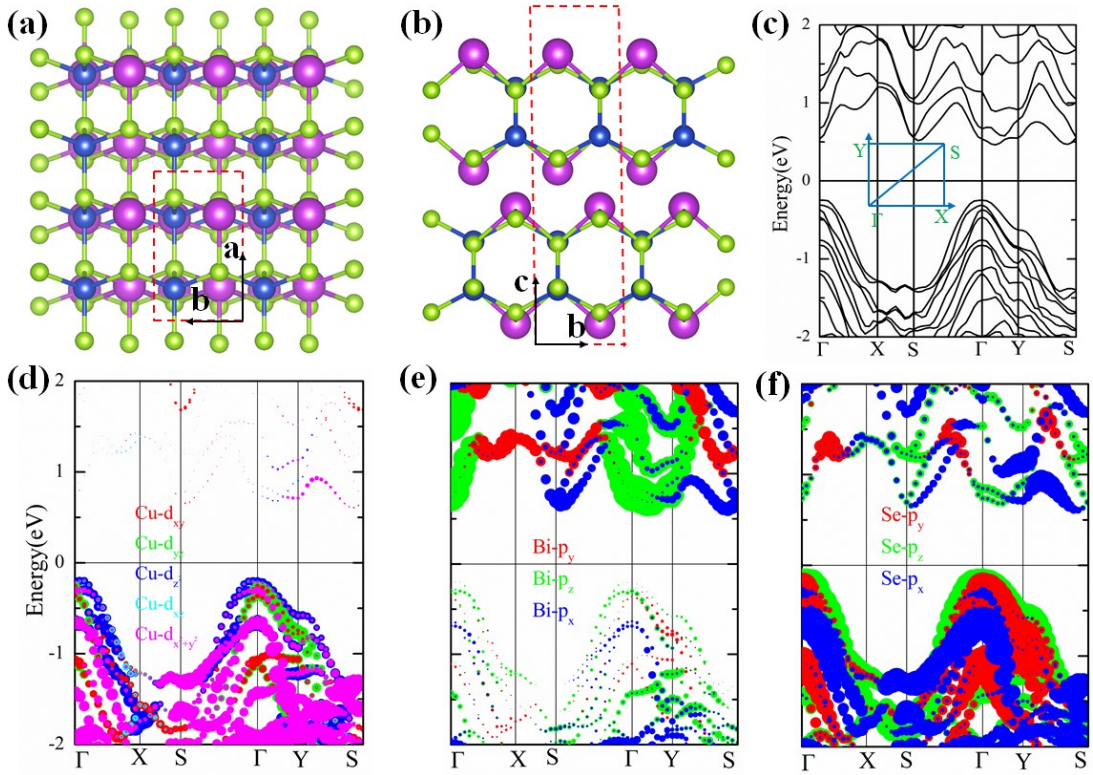


**Figure S10.** The structure, band structure, and atomic orbitals of the bilayer $CuBiSe_2$. (a) and (b) are the top and side views respectively. (c)HSE energy band structure calculations (see the blue inset for the high symmetrical K-points) with the spin-orbit coupling and Van der Waals interactions, where the Fermi level has been set to 0 eV. (d), (e) and (f) are atomic orbital projected band structures in Cu, Bi, Se atoms respectively. The Cu, Bi, Se atoms are shown as blue, purple and green spheres, respectively.

## 6. Carrier mobilities.

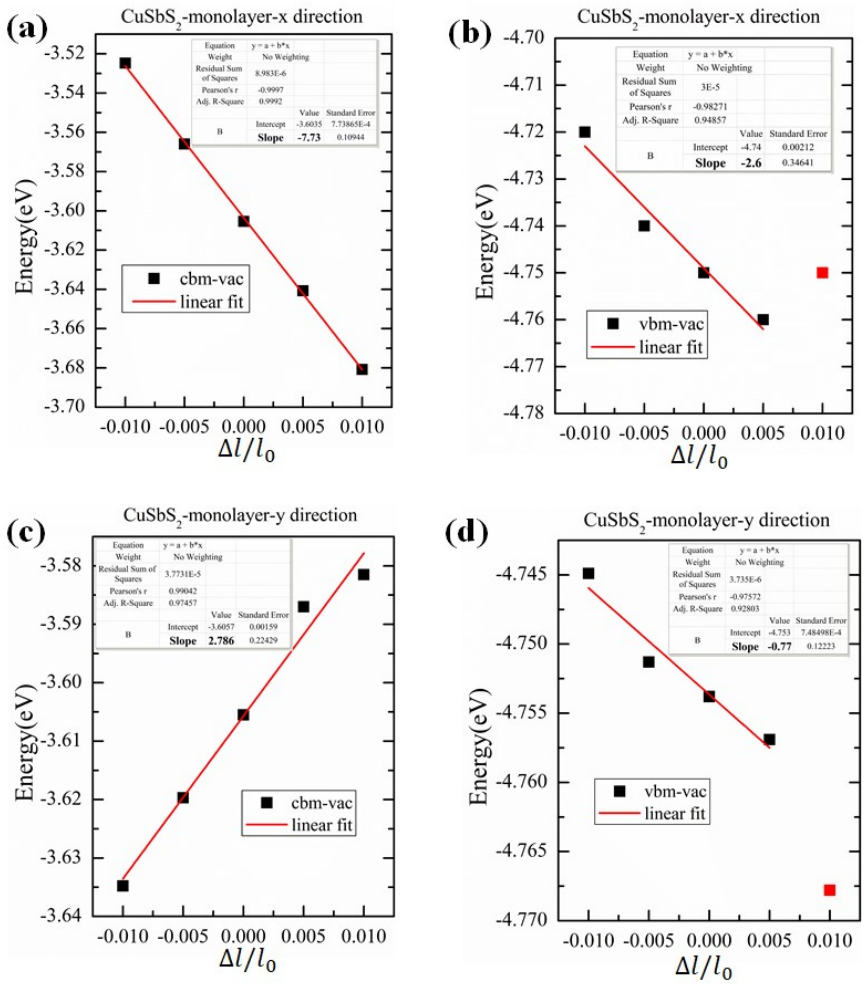


**Figure S11.** The slopes of (a) and (b) are respectively the deformation potential constants of the electron and hole of $CuSbS_2$ along the x direction, (c) and (d) are the deformation potential constants of the electron and hole of $CuSbS_2$ along the y direction respectively. The 'vbm-vac' means the VBM minus the vacuum level, and the 'cbm-vac' means the CBM minus the vacuum level. The red dots of (b) and (d) deviate more, so these data are omitted.

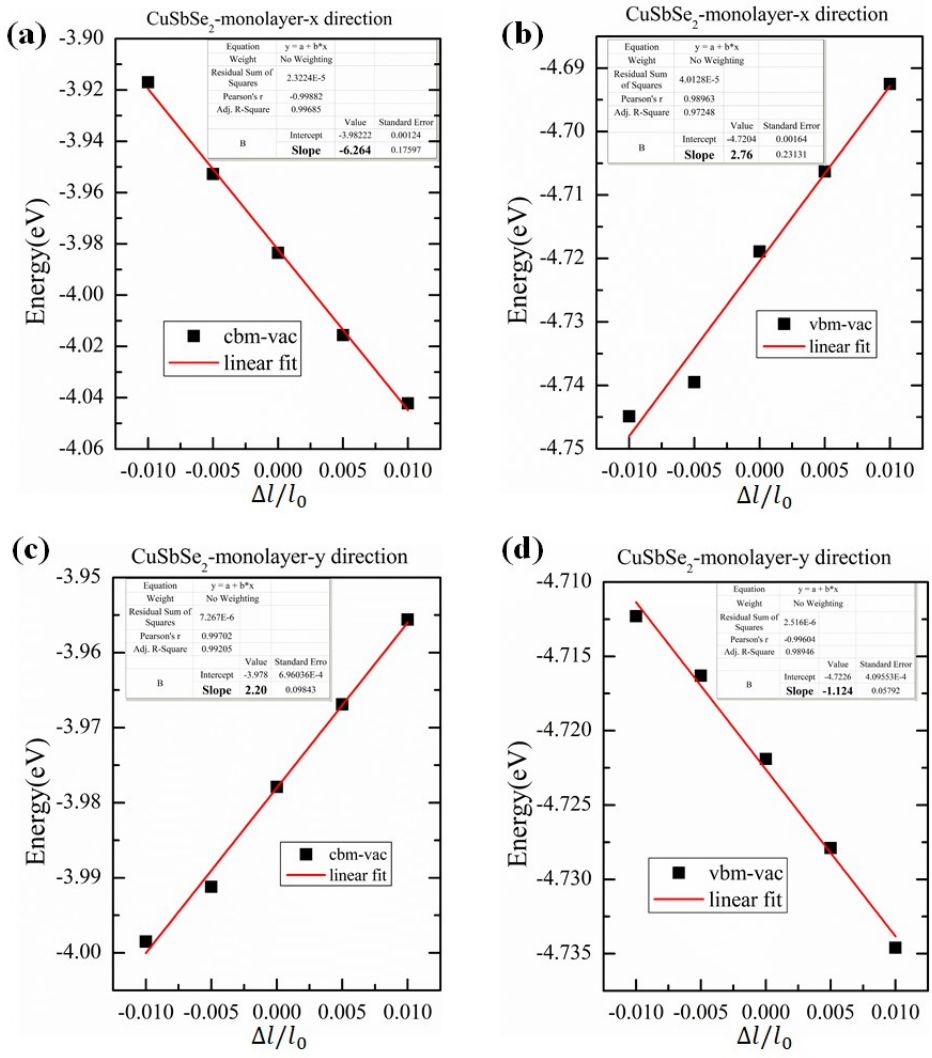


**Figure S12.** The slopes of (a) and (b) are respectively the deformation potential constants of the electron and hole of $CuSbSe_2$ along the x direction, (c) and (d) are the deformation potential constants of the electron and hole of $CuSbSe_2$ along the y direction respectively. The 'vbm-vac' means the VBM minus the vacuum level, and the 'cbm-vac' means the CBM minus the vacuum level.

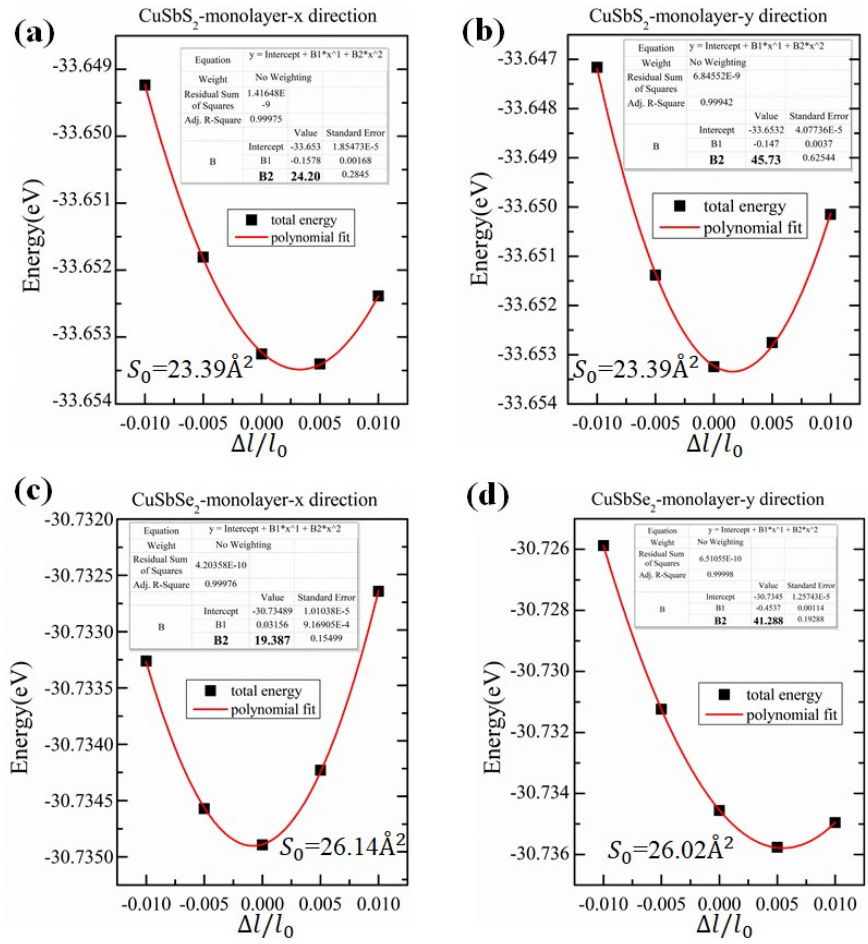


**Figure S13.** (a) and (b) are the fitting of the total energies of $CuSbS_2$ as functions of in-plane strains along the x direction and the y direction respectively, (c) and (d) are the fitting of the total energies of $CuSbSe_2$ as functions of in-plane strains along the x direction and the y direction respectively. $S_0$ denotes the in-plane area under equilibrium.

| materials | $m_x^*(m_0)$ | $m_y^*(m_0)$ | $E_{1x}(J\cdot10^{-19})$ | $E_{1y}(J\cdot10^{-19})$ | $C_{2D-x}(J/m^2)$ | $C_{2D-y}(J/m^2)$ | $\mu_{2D-x}(cm^2/(V\cdot s))$ | $\mu_{2D-y}(cm^2/(V\cdot s))$ |
|---|---|---|---|---|---|---|---|---|
| $CuSbS_2$(electron) | 0.25 | 2.49 | 12.37 | 4.46 | 33.12 | 62.56 | 59.94 | 87.44 |
| $CuSbS_2$(hole) | 0.67 | 0.85 | 4.16 | 1.23 | 33.12 | 62.56 | 208.3 | 3547.56 |
| $CuSbSe_2$(electron) | 0.27 | 2.25 | 10.02 | 3.52 | 23.74 | 50.78 | 61.41 | 127.72 |
| $CuSbSe_2$(hole) | 0.52 | 0.72 | 4.42 | 1.8 | 23.74 | 50.78 | 209.52 | 1951.68 |

**Table S1.** The carrier mobility of monolayer $CuSbCh_2$(Ch=S, Se) with direct bandgaps using the deformation potential with formula $\mu_{2D} = \frac{e\hbar^3 C_{2D}}{k_B T m^* m_d E_1^2}$ [1-4], where $\frac{e\hbar^3}{k_B T} \sim 4.539 \times 10^{-101}\ C\cdot J^2\cdot s^3$; $m_d$, defining $m_d = \sqrt{m_x^* m_y^*}$, is the average effective mass of the carrier; $k_B$ is Boltzmann's constant; $E_1$, which is defined as $E_1 = \frac{\Delta E}{\Delta(\frac{\Delta l}{l_0})}$, denotes the deformation potential constant of hole or electron along the direction of transmission; $C_{2D} = \frac{2}{S_0} \times \frac{\partial^2 E}{\partial(\frac{\Delta l}{l_0})^2}$ the crystal's the elastic modulus. $m^*$ denotes the effective mass along the direction of transmission. $\Delta E$ is the energy change of CBM or VBM under in-plane compression or tensile strain; $l_0$ is the equilibrium lattice constant in the direction of transmission, and $\Delta l$ is the deformation of $l_0$. $S_0$ denotes in-plane area under equilibrium. $m_0$ denotes electron mass with value of $9.11 \times 10^{-31}$kg. $\mu_{2D}$ denotes carrier mobility. Temperature T is set to 300 K. The unit $1V = 1J/C$.

**7. Bandgaps calculated by PBE/HSE with/without SOC between monolayer and bilayer $CuMCh_2$(M=Sb, Bi; Ch=S, Se).**

| function | PBE+VdW | | | | | | | |
|---|---|---|---|---|---|---|---|---|
| layers | $CuSbS_2$ | $CuSbS_2$+SOC | $CuSbSe_2$ | $CuSbSe_2$+SOC | $CuBiS_2$ | $CuBiS_2$+SOC | $CuBiSe_2$ | $CuBiSe_2$+SOC |
| monolayer-bandgap(eV) | 0.41 | 0.40 | 0.21 | 0.19 | 0.34 | 0.26 | 0.19 | 0.14 |
| bilayer-bandgap(eV) | 0.6 | 0.58 | 0.3 | 0.27 | 0.47 | 0.39 | 0.27 | 0.21 |

**Table S2.** The bandgaps obtained using PBE functionals with/without the SOC effects and all data consider Van der Waals interactions.

| function | HSE+VdW | | | | | | | |
|---|---|---|---|---|---|---|---|---|
| layers | $CuSbS_2$ | $CuSbS_2$+SOC | $CuSbSe_2$ | $CuSbSe_2$+SOC | $CuBiS_2$ | $CuBiS_2$+SOC | $CuBiSe_2$ | $CuBiSe_2$+SOC |
| monolayer-bandgap(eV) | 1.18 | 1.16 | 0.89 | 0.81 | 1.00 | 0.88 | 0.73 | 0.53 |
| bilayer-bandgap(eV) | 1.37 | 1.35 | 0.99 | 0.95 | 1.08 | 1.00 | 0.81 | 0.71 |

**Table S3.** The bandgaps obtained using HSE functionals with/without the SOC effects and all data consider Van der Waals interactions.

## 8. The bandgaps changes from $CuSbS_2$/$CuBiS_2$ monolayer to $CuSbS_2$-$CuBiS_2$ Van der Waals heterojunction.

| | Monolayer-$CuSbS_2$ | Monolayer-$CuBiS_2$ | Hetero-$CuSbS_2$ | Hetero-$CuBiS_2$ |
|---|---|---|---|---|
| bandgap(eV) at Γ point | 1.13 | 0.98 | 1.23 | 1.33 |

**Table S4.** The bandgaps in $CuSbS_2$/$CuBiS_2$ monolayer and $CuSbS_2$-$CuBiS_2$ Van der Waals heterojunction.

## 9. Hopping integrals

**Table S5.** Orbital hopping integrals in the bilayer $CuSbSe_2$, where $Se^{(4)}$-$p_z$ indicates the $p_z$ orbital of the fourth selenium atom (other atomic orbitals symbol deduced by analogy). The unit is eV.

| $CuSbSe_2$ hopping integrals | |
|---|---|
| Orbitals | $Sb^{(4)}$-$p_z$ |
| $Se^{(4)}$-$p_z$ | 0.70 |
| $Se^{(4)}$-$p_y$ | -0.87 |
| $Cu^{(2)}$-$d_z{}^2$ | -0.39 |
| $Sb^{(3)}$-$p_z$ | 0.14 |

**Table S6.** Orbital hopping integrals in the bilayer $CuBiS_2$, where $S^{(1)}$-$p_z$ indicates the $p_z$ orbital of the first sulfur atom (other atomic orbitals symbol deduced by analogy). The unit is eV.

| $CuBiS_2$ hopping integrals | |
|---|---|
| Orbitals | $Bi^{(2)}$-$p_z$ |
| $S^{(1)}$-$p_z$ | 0.71 |
| $S^{(1)}$-$p_y$ | -0.89 |
| $Cu^{(4)}$-$d_z^2$ | -0.43 |
| $Bi^{(1)}$-$p_z$ | 0.15 |

**Table S7.** Orbital hopping integrals in the bilayer $CuBiSe_2$, where $Se^{(1)}$-$p_z$ indicates the $p_z$ orbital of the first selenium atom (other atomic orbitals symbol deduced by analogy). The unit is eV.

| $CuBiSe_2$ hopping integrals | |
|---|---|
| Orbitals | $Bi^{(2)}$-$p_z$ |
| $Se^{(1)}$-$p_z$ | 0.69 |
| $Se^{(1)}$-$p_y$ | -0.88 |
| $Cu^{(4)}$-$d_z^2$ | -0.43 |
| $Bi^{(1)}$-$p_z$ | 0.11 |

## REFRENCES


(1) J. Bardeen, W. Shockley. Physical Review, 1950, 80, 72-80.

(2) J. Qiao, X. Kong, Z. X. Hu, F. Yang, W. Ji, Nat. Commun. 2014, 5, 4475.

(3) S. Bruzzone, G. Fiori, Appl. Phys. Lett. 2011, 99, 222108.

(4) R. Fei, A. Faghaninia, R. Soklaski, J. A. Yan, C. Lo, L. Yang, Nano Lett. 2014, 14, 6393 −6399.